

A multi-scale analytical model for the performance of a tidal stream array in a tidal channel

F. He, Y.L. Chen, A. Angeloudis, C.R. Vogel and T. A.A. Adcock

Abstract—Assessing the tidal resource is central to the feasibility analysis of any development of tidal stream turbines. This is true for the CoTide project which seeks to optimise the design of tidal stream turbines by building an integrated design tool considering hydrodynamics, structural effects, fatigue, environmental impact, etc. However, there is no closed-form analytical solution for the tidal resource assessment. Motivated by this, this paper proposes a multi-scale framework for tidal resource assessment for the Co-Tide project. The key element of this framework is to model the system, i.e. an array of turbines (arranged in a row) partially occupying a tidal channel, at different scales (channel-scale, array-scale, turbine-scale), and then coupling them together through the net resistance of the turbine array solved by a drag model that might be derived from laboratory experiments or numerical simulations. The channel-scale flow dynamics is described by the Garrett & Cummins (2005) model [1] whereas based on the scale separation model of Nishino & Willden (2012) [2] the array-scale and turbine-scale flows are modelled separately by the Garrett & Cummins (2007) model [3] and then coupled together. Using characteristics representative of a tidal site (including tidal flow characteristics, channel geometry and turbine geometry) as inputs, we have employed the framework to predict the velocity in the channel, velocity through the array and the power generated by the array over time. Only two principal tidal constituents are considered here as increasing the number of tidal constituents significantly increases the computational cost. The model can be adapted for other tidal energy projects and has flexibility to incorporate more detailed sub-models in future.

Index Terms—Co-Design, Tidal stream resource, Tidal turbine array

I. INTRODUCTION

The CoTide project aims to use a co-design methodology to improve the design of tidal stream energy systems. The project will optimise across multiple aspects of the design including turbine performance, environmental impact, fatigue, sustainability of materials, etc. Critical to this is, of course, the “resource model”. This must take the environmental flow conditions and understand how the presence of a tidal turbine farm

alters the flow. The power, thrust, and other parameters can then be calculated. Given this will be used as part of a complex optimisation routine, computational efficiency is paramount. Thus, the goal of this work is to develop a framework for resource assessment that is accurate enough for co-design to take place but computationally fast enough to enable optimisation.

Resource assessment in tidal stream energy is a complex problem (see discussion in the review paper [4]). Due to the highly multi-scale nature of the problem we must rely on computational modelling with few developments on experimental modelling since a 2013 EWTEC paper [5]. Resource assessment is carried out using flow models which solve the depth-averaged shallow water equations (for example [6]–[8]) with some modellers extending the analysis to three dimensions [9], [10]. However, such modelling is computationally expensive making it impractical to use as part of an optimisation routine. Therefore simpler analytical models would be ideal for the present purpose, which are computationally efficient but can capture the physics that is critical for the co-design process.

To evaluate a channel’s potential for tidal stream power generation, to a first approximation, the leading-order flow dynamics at generic sites can be analytically modelled by tidal flow through a row of turbines partially occupying a rectangular channel (see Figure 1). There are three different scales of flows in this problem, i.e. channel-scale (Figure 1a), array-scale (Figure 1c) and turbine-scale (Figure 1d). At the channel-scale, the tidal flow through a channel is controlled by a momentum balance between the tidal driving head and the resistance provided by both the bed friction and the turbine thrust. Integrating the momentum equation describing this momentum balance along the channel leads to the channel-scale model of Garrett & Cummins (2005) [1]. This model has been widely used to analyse the characteristics of the tidal resource [11]–[15]. This model is a substantial simplification of the complex dynamics typically present at a real site [16]. However, it is possible to adopt this model provided that the goal here is not to model a real site, but rather to capture the leading-order dynamics of generic sites for which the model is capable.

In comparison to this, at the array-scale, the turbines within the array as a combination will offer net resistance to the flow, which results in a portion of incoming flow diverting around the array (bypass flow), with the rest passing through the array (core flow). Taking the

© 2025 European Wave and Tidal Energy Conference. This paper has been subjected to single-blind peer review.

The authors are funded by the EPSRC CoTide project (EP/X03903X/1).

Authors F. He, C.R. Vogel and T.A.A Adcock are affiliated with the Department of Engineering Science, University of Oxford, Oxford OX1 3PJ, United Kingdom (email: fei.he@eng.ox.ac.uk)

Authors Y.L. Chen and A. Angeloudis are affiliated with School of Engineering, Institute for Infrastructure and the Environment, The University of Edinburgh.

Digital Object Identifier:

<https://doi.org/10.36688/ewtec-2025-paper-977>

whole array as a porous obstruction, it is then possible to adopt the model of Garrett & Cummins (2007) [3] to describe flow through the porous array. Similarly, at the turbine-scale, a single turbine behaves as a porous obstruction, again, the model of Garrett & Cummins (2007) [3] can be used to characterise flow through the single turbine within the array.

Application of the model of Garrett & Cummins (2007) [3] to array-scale and turbine-scale flows simultaneously, however, requires the scale separation model that was proposed in Nishino & Willden (2012) [2]. Specifically, it is assumed in this model that turbine-scale mixing, between the turbine core and bypass flows, scales on the turbine diameter d and occurs ahead of the start of array scale mixing, between the array core and bypass flows, which scales on the width of the array W_A (see Figure 1c, d). This allows for the array-scale and turbine-scales stream tubes (indicated by blue dot-dashed line and dashed line in Figure 1c, d) to expand along the channel to reach the equilibrium of pressures between the core and the bypass flows at each scale before mixing between each two streams. Accordingly, the model of Garrett & Cummins (2007) [3] can be applied to array-scale and turbine-scale flows simultaneously. Combining this scale separation model [2] with the model of Garrett & Cummins (2007) [3] and the model of Garrett & Cummins (2005) [1], it is then possible to evaluate efficiency of an array of turbines in a channel for a given local and array blockage ratios and wake induction factor for individual turbines as described in Dehtyriov et al. (2023) [17] (see also [18]).

Practically, this wake induction factor (equivalently the thrust coefficient for the turbine) is unknown *a priori*. Therefore, coupling these three models above does not lead to a closed-form solution to this problem in terms of predicting power generation for a general array of turbines in a channel. In this paper, a drag model that relates the thrust coefficient to the incident flow velocity is introduced to close this problem. Integrating these three models with the drag model leads to a tidal resource assessment framework. The primary aim of this paper is to apply this framework with practical site characteristics to conduct resource assessment.

II. MULTI-SCALE MODEL FRAMEWORK

In this section, we introduce a multi-scale framework for tidal resource assessment for the Co-Tide project, which models the system at different scales (channel-scale, array-scale, turbine-scale) and then couple them together through the net resistance of the turbine array.

A. Channel-scale model

To establish the integrated framework, we start by introducing the one-dimensional channel dynamics model of Garrett & Cummins [1], which takes the form of

$$\frac{\partial U_C}{\partial t} = \frac{g\Delta\eta}{L} - \frac{1}{2} \left(\frac{C_D}{h} + \frac{B_A C_A}{L} \right) U_C |U_C|, \quad (1)$$

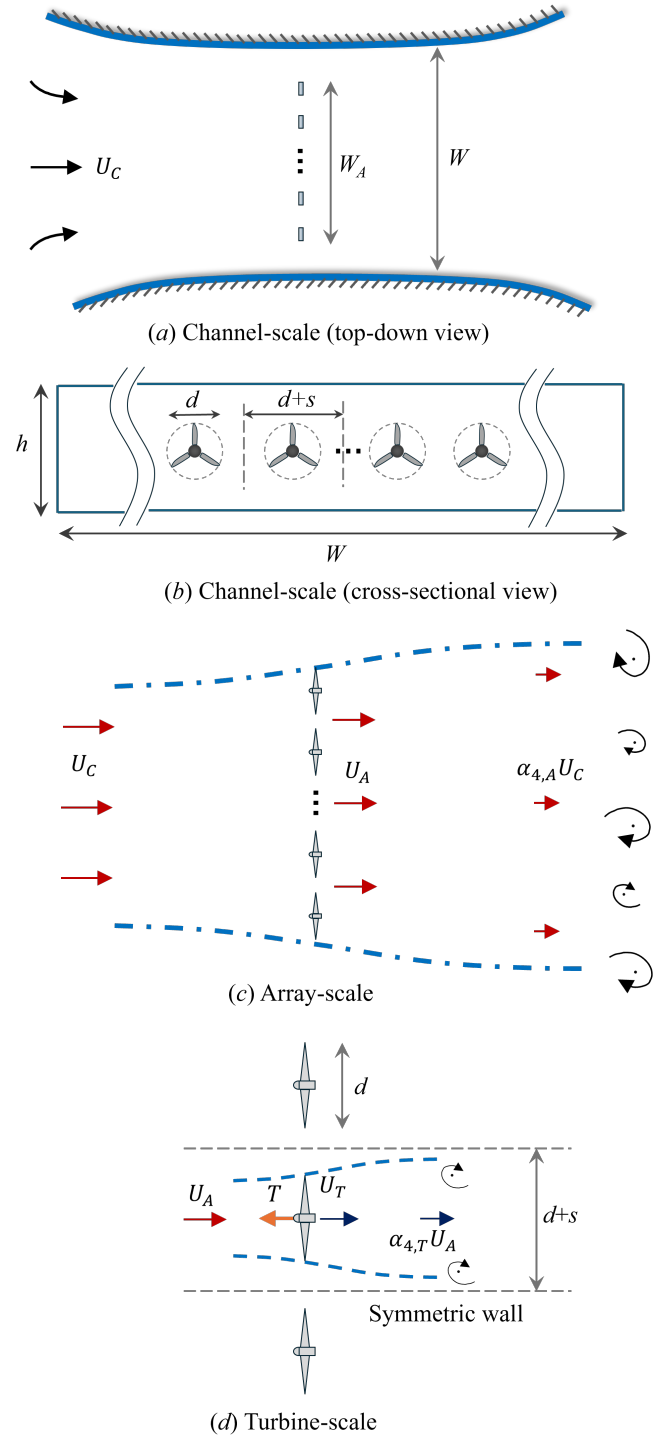


Fig. 1. Sketch of multi-scale dynamics in tidal flow through a row of turbines in a channel. The channel in (a, b) has length L , width W , and water depth h , whereas the turbine has diameter d and spacing (tip-to-tip) between adjacent turbines s . The flow diversion around the entire array is laterally bounded by the physical channel wall, where the flow diversion around each turbine is laterally bounded by local symmetry of the flow (gray dashed line in (b, d)). Through a momentum balance between the tidal driving force, the bed shear and the turbine array thrust, the tidal current velocity is U_C upstream of the turbine array in (a), and then reduced to $\alpha_{2,A} U_C$ due to the flow blockage of the turbine array, before further reduction to $\alpha_{4,A} U_C$ in the array wake due to the expansion of streamtube bounding the array (dot-dashed line in (c)). This core-velocity of $\alpha_{2,A} U_C$ sets the incident velocity for each turbine, which is reduced to $U_T = \alpha_{2,T} U_A$ when passing through it, before further reduction to $\alpha_{4,T} U_A$ in the turbine wake.

where U_C is the along-channel velocity, t is the time, g is the gravitational constant, $\Delta\eta$ is the difference in

surface elevation between the two ends of the channel, L is the channel length, C_D is the bed friction coefficient, h is the water depth, C_A is the thrust coefficient for the total array, defined as

$$C_A = \frac{T_A}{\frac{1}{2}\rho U_C^2 A}, \quad (2)$$

in which T_A is the thrust acting on the turbine array, ρ is the fluid density (1025 kg m^{-3}), A is the cross-sectional area of the turbine array, and B_A is the channel blockage ratio of the array defined as

$$B_A = \frac{A}{hW} = \frac{hn(d+s)}{hW}, \quad (3)$$

where n is the number of turbines in a row, d is the turbine diameter, and s is the (tip-to-tip) gap distance between adjacent turbines (see Figure 1b).

B. Scale separation model

To evaluate the efficiency of a partial tidal fence, i.e. a row of a number of turbines arrayed only across a part rather than the entire cross-section of a wide channel, the scale-separation model was developed in Nishino & Willden (2012) [2]. Assumptions for this model are detailed below.

In this model, firstly, it was assumed that the two scales of flows are separated. This assumption of scale separation implicitly requires that the turbine fence is sufficiently wide (large enough number of turbines n) to allow turbine-scale mixing, between the turbine core and bypass flows, which scales on the turbine diameter d to occur before the start of array scale mixing, between the array core and bypass flows, which scales on the length of the array W_A (see Figure 1a, b). This requirement essentially ensures that for both the array and the turbine the core flow expands and the bypass flow contracts freely downstream until a point where static pressure equilibrium between the core and bypass streams is reached. This allows for application of the Garrett & Cummins (2007) model [3] to array-scale and turbine-scale flows independently (introduced below in section C).

Secondly, individual turbines are assumed to be operated in the same local flow condition, i.e. the same core flow velocity through each turbine. This means that the thrusts on individual turbines are identical across the array.

Thirdly, the channel is sufficiently long – multiples of the array width W_A – for array-scale mixing to be completed within the channel. The numerical simulations of Nishino & Willden (2013) [19] suggest that the restriction on the number of turbines to achieve scale separation is not particularly onerous, with $n \geq 8$ achieving good agreement between theory and numerical simulation.

C. Array-scale, turbine-scale model

The Garrett & Cummins (2007) model [3] describes flow through a porous disc mathematically representing a porous obstruction in a channel. Here, the porous

obstruction can be the entire array or a single turbine. This model extends the well-known actuator disc theory of Lanchester (1915) [20], Betz (1920) [21] and Joukowski (1920) [22] applied conventionally to an infinitely wide channel where the bypass flow can expand freely to a case of a porous disc in a channel with finite width where the expansion of the bypass flow is confined by the sidewall. The key element of this theory is to relate the velocity through the disc to the thrust on the disc by applying mass, energy, and momentum conservation to different parts of the flow field.

Starting with the array-scale problem, application of the Garrett & Cummins (2007) model [3] to the entire array gives

$$C_A = (1 - \alpha_{4,A}) \left[\frac{(1 + \alpha_{4,A}) - 2B_A\alpha_{2,A}}{(1 - B_A\alpha_{2,A}/\alpha_{4,A})^2} \right], \quad (4)$$

in which the array wake induction factor $\alpha_{4,A}$ is the ratio of array wake velocity (at the array scale pressure recovery location) to the upstream channel velocity U_C , which is related to the array core velocity factor $\alpha_{2,A}$ by

$$\alpha_{2,A} = \frac{1 + \alpha_{4,A}}{(1 + B_A) + \sqrt{(1 - B_A)^2 + B_A(1 - 1/\alpha_{4,A})^2}}, \quad (5)$$

Once the array blockage B_A has been specified, (4) and (5) may be solved for C_A as a function of $\alpha_{4,A}$ alone. For each $0 < \alpha_{4,A} < 1$, (5) provides a unique solution $0 < \alpha_{2,A} < 1$, which then solves for a unique C_A in (4).

Following Nishino & Willden (2012) [2], we then apply the Garrett & Cummins (2007) model [3] to the turbine-scale problem, yielding a similar form of equations that relate the turbine thrust coefficient C_T to the turbine induction factor $a_{2,T}$, which itself relates the core flow velocity through the turbine to the array core velocity through $U_T = a_{2,T}U_A$. Once the turbine blockage B_T has been specified, the array thrust C_T is parametrised by $a_{2,T}$ as

$$C_T = (1 - \alpha_{4,T}) \left[\frac{(1 + \alpha_{4,T}) - 2B_T\alpha_{2,T}}{(1 - B_T\alpha_{2,T}/\alpha_{4,T})^2} \right], \quad (6)$$

where $\alpha_{4,T}$ is the ratio of the turbine-scale wake velocity (at the device-scale pressure equilibrium location) to the turbine approach velocity U_A , and B_T is the local blockage ratio defined as

$$B_T = \frac{\pi d^2/4}{(d+s)h}, \quad (7)$$

where the denominator is the cross-sectional area of the 'local' channel with symmetry walls for the passage of the turbine-scale flow. The turbine induction factor is defined as

$$a_{2,T} = \frac{1 + \alpha_{4,T}}{(1 + B_T) + \sqrt{(1 - B_T)^2 + B_T(1 - 1/\alpha_{4,T})^2}}, \quad (8)$$

The turbine-scale and array-scale problems are coupled kinematically through the array approach velocity U_A , and dynamically through specifying the array thrust to be n times the turbine thrust, i.e. $T_A = nT_D$, or non-dimensionally,

$$C_A = (\alpha_{2,A})^2 B_A C_T, \quad (9)$$

The kinematic and dynamic coupling closes the partial fence problem leading to a solution for array thrust as a function of the turbine thrust coefficient C_T .

Finally, following Garrett & Cummins (2007) [3], we neglect changes in the free surface elevation and assume that the array-scale and turbine-scale flows are bounded by a rigid lid. However, at the channel scale, following Garrett & Cummins (2005), we assume that the channel depth varies in time according to the driving tidal forcing. Relaxation of the rigid-lid assumption at the turbine and array scales has a significant impact only on the model predictions for large Froude number ($Fr = U_C/\sqrt{gh}$) channels or high global blockage ratios ($B_A B_T$) [23]. However, as Froude numbers for realistic tidal channels are comparatively low ($0.1 \leq Fr \leq 0.2$) [23], and the results presented herein show peak performance points at modest global blockage ratios, the rigid-lid assumption made here will introduce only small errors for practical turbine array deployment scenarios.

D. Drag model

Once the the local blockage ratio for the turbine B_T and the channel blockage ratio for the array B_A are determined, coupling of the channel-scale model [1], the scale separation model [2] and the array-scale and turbine-scale model [3] gives a solution for the efficiency of a row of turbines in a channel with a presumed array induction factor $\alpha_{2,A}$ in the range of 0-1, as described in Dehtyriov et al. (2023) [17]. However, in practice, this array induction factor is unknown *a priori*.

To close this problem, a drag model is introduced. The drag model can be obtained through laboratory experiments or numerical simulations, and relates the incident flow velocity for a single turbine to the thrust of the turbine. Here, we adopt a drag model of the form

$$C_T = \begin{cases} 0.96, & U_A \leq U_r \\ 0.96 \left(\frac{U_r}{U_A} \right)^2, & U_A > U_r \end{cases}, \quad (10)$$

where U_r is rated velocity above which the turbine thrust is reduced by, for example, pitching the blades, selected here to be 2.0 m/s. Note that in turbine simulations and experiments, the incident flow velocity for a single turbine is equivalent to the channel free-stream velocity U_C . i.e. array-scale deceleration of the incident flow does not occur. However, in multi-turbine configurations, the flow incident on an individual turbine is not U_C but rather is U_C corrected by a factor of $\alpha_{2,A}$, i.e. $\alpha_{2,A}U_C$, due to array-scale hydrodynamics.

E. Integrated framework

Integrating the four models above provides a closed-form solution to the system, which leads to an integrated framework for assessing power generation for a row of turbines in a rectangular channel. The input for this framework includes tidal characteristics (period, neap/spring velocities), turbine diameter, and channel geometry (channel length, channel width, water depth) based on site data. With these inputs, unknown variables for this analytical framework, e.g. $\alpha_{2,A}, C_A, C_T, U_C$ can be solved by running the four models iteratively.

III. TIDAL CONSTITUENTS

Tides are generally modelled using harmonic constituents based on the methods developed by Doodson [24]. There are a range of tidal constituents including diurnal (K_1, O_1), semidiurnal (M_2, S_2, N_2, K_2) and higher order constituents (M_4) [25]. However, in many locations around the world, the tides are dominated by the principal M_2 and s_2 constituents, modulating with each other to form neap and spring tides. This is particularly true for many sites which are of interest to tidal stream power developers because the areas with the largest tides are typically locations where the bathymetry leads to amplification of these constituents (for example, the west coast of the UK, and the Bay of Fundy, North America) [12]. The presence of multiple constituents results in variability of daily average power by tidal turbines over the entire neap/spring cycle and indeed over the whole 19.6 year idal cycle [26], [27]. However, incorporating these secondary tidal constituents in tidal resource assessment requires a long-time assessment, which is computationally expensive. This is even be a problem for the Co-Tide project for which the aim is to optimise the tidal energy systems across multiple aspects. Therefore, in this study, we consider two principal constituents, i.e. M2 and S2 while demonstrating how the increase of tidal constituents can significantly increase computational costs.

IV. RESULTS

A. Evaluate performance of a row of turbines in a channel

The power generation for candidate tidal channels is directly related to the amplitude and phase of the principal tidal constituents driving the flow through the channel. Assuming two principal constituents, the elevation difference across the channel $\Delta\eta$ can be written as

$$\Delta\eta = a_{M2} \sin(\omega_{M2}t) + a_{S2} \sin(\omega_{S2}t), \quad (11)$$

where a_{M2} and a_{S2} are amplitudes of tidal force components, and ω_{M2} and ω_{S2} are the frequencies of the M_2 and S_2 constituents respectively.

In practice, the tidal forcing amplitudes, a_{M2} and a_{S2} , are unknown for real candidate sites. However, it is possible to conduct field measurements to obtain the time history of tidal velocity and then calculate the time-mean values of neap and spring tide velocities.

With these time-mean values, it is then straightforward to back-calculate the amplitudes of tidal forcing. This back calculation is very important for tidal resource assessment due to the channel-scale flow dynamics. Specifically, the turbine thrust is capable of affecting the tidal velocity in a channel as shown in equation (1) [1]. The dependence of the tidal velocity in a channel on the turbine thrust suggests that it is not possible to rely on the field measurements of tidal velocity in an empty channel (without turbines) to conduct tidal resource assessment (with turbines), as once turbines are deployed in the turbine and channel velocity is altered. However, it is reasonable to assume that the tidal forcing is not influenced by the channel dynamics [1]. Therefore, once the back calculation is done for an empty channel, the tidal forcing term in the in the Garrett & Cummins model [1] remains constant regardless of the number of turbines deployed in the channel, which serves for tidal resource assessment for varying numbers of turbines.

An approach for predicting the tidal forcing amplitudes, a_{M2} and a_{S2} based on field measurements of time-mean neap and spring tidal velocities is introduced here. We start by substituting (11) into (1) and omitting the turbine thrust term for an empty channel, which gives

$$\frac{\partial U_C}{\partial t} = \frac{g}{L} (a_{M2} \sin(\omega_{M2}t) + a_{S2} \sin(\omega_{S2}t)) - \frac{1}{2} \frac{C_D}{h} |U_C| U_C, \quad (12)$$

Neglecting the bed friction term in (12) yields

$$\frac{\partial U_C}{\partial t} = \frac{g}{L} (a_{M2} \sin(\omega_{M2}t) + a_{S2} \sin(\omega_{S2}t)), \quad (13)$$

Taking the integral of (13) at both sides leads to

$$U_C(t) = -\frac{g}{L} \left[\frac{a_{M2}}{\omega_{M2}} \cos(\omega_{M2}t) + \frac{a_{S2}}{\omega_{S2}} \cos(\omega_{S2}t) + c \right], \quad (14)$$

Assuming the time-mean value of U_C to be equal to zero gives $c = 0$. With this, rearranging (14) leads to

$$U_C(t) = -\frac{g}{2L} \left(\frac{a_{M2}}{\omega_{M2}} + \frac{a_{S2}}{\omega_{S2}} \right) [\cos(\omega_{M2}t) + \cos(\omega_{S2}t)] - \frac{g}{2L} \left(\frac{a_{M2}}{\omega_{M2}} - \frac{a_{S2}}{\omega_{S2}} \right) [\cos(\omega_{M2}t) - \cos(\omega_{S2}t)], \quad (15)$$

From (15), the time-mean spring (maximum) and neap (minimum) velocities are

$$\overline{U_{spring}} = \frac{g}{L} \left(\frac{a_{M2}}{\omega_{M2}} + \frac{a_{S2}}{\omega_{S2}} \right), \quad (16)$$

$$\overline{U_{neap}} = \frac{g}{L} \left(\frac{a_{M2}}{\omega_{M2}} - \frac{a_{S2}}{\omega_{S2}} \right), \quad (17)$$

where the overbar represent a long-time averaging operation.

We can then determine the tidal forcing amplitudes a_{M2} and a_{S2} based on (16) and (17) once field measurements of $\overline{U_{spring}}$ and $\overline{U_{neap}}$ are obtained. This only

provides an initial guess for the real values of a_{M2} and a_{S2} as we neglect the bed friction term in (15) that acts as a damping term on the tidal velocity in a channel. However, it is straightforward to evaluate the more accurate values including drag effects by numerically solving (15) starting with the initial theoretical guess. For instance, for time-mean spring and neap tidal velocities (3.2, 1.6 m/s), a water depth $h = 25$ m and channel length $L = 7000$ m, the two tidal forcing amplitudes are determined as

$$a_{M2} = 0.495, a_{S2} = 0.268, \quad (18)$$

Substituting these tidal forcing amplitudes into (12), it is then possible to conduct tidal resource assessment for a row of turbines in a channel based on the integrated framework.

Here, we assume $n = 5$, a turbine diameter of 10.8 m, and channel dimensions of $h = 25$ m, $W = 2000$ m, $L = 7000$ m, and time-mean spring and neap tidal velocities (3.2, 1.6 m/s).

Figure 2 demonstrates the predictive capability of this integrated framework. Firstly, the time history of channel velocity U_C in Figure 2a. As expected, the velocity through the turbine array U_A is lower than U_C (comparing Figure 2a and 2b) especially around the spring tide. The ratio between the two velocities, i.e., the array induction factor $\alpha_{2,A}$, varies with time as discussed below. Around the neap tide, the velocity through the array U_A is less than the rated velocity $U_r = 2.0$ m/s. Below this speed, each turbine has a constant thrust coefficient with $C_T = 0.96$, which leads to a constant thrust coefficient for the array C_A and hence constant array induction factor $\alpha_{2,A} = 0.91$ (see Figure 2c).

When the flow evolves into spring tide, for a period of time in each oscillating cycle, the velocity through the array U_A is greater than the rated velocity U_r . The thrust coefficient of individual turbines is reduced accordingly as described in equation (10), for example, by pitching the blades. This results in an increase in array induction factor, which exhibits an oscillatory pattern with increasing amplitude of $\alpha_{2,A}$ over time and eventually reaching the highest peak of 0.95. This value is higher than that of 0.91 in the neap tide. It highlights how the rated velocity influences the turbine-scale, channel-scale, and array-scale flow dynamics.

The thrust on individual turbines shows distinct features between neap and spring tides (see Figure 2d). When the flow evolves from neap to spring tide before U_A reaches the rated velocity, the thrust on each turbine increases with a constant thrust coefficient and proportional to the tidal velocity squared through the array. Once the velocity through the array reaches U_r , the thrust on each turbine is capped rather than continuously increasing further with the velocity U_A .

Finally, there is a large difference in power generation between the neap and spring tides (see Figure 2e). The peak power for a row of 5 turbines can reach approximately 9.3 MW in the spring tide but is reduced to almost zero at the neap tide (see Figure 2e).

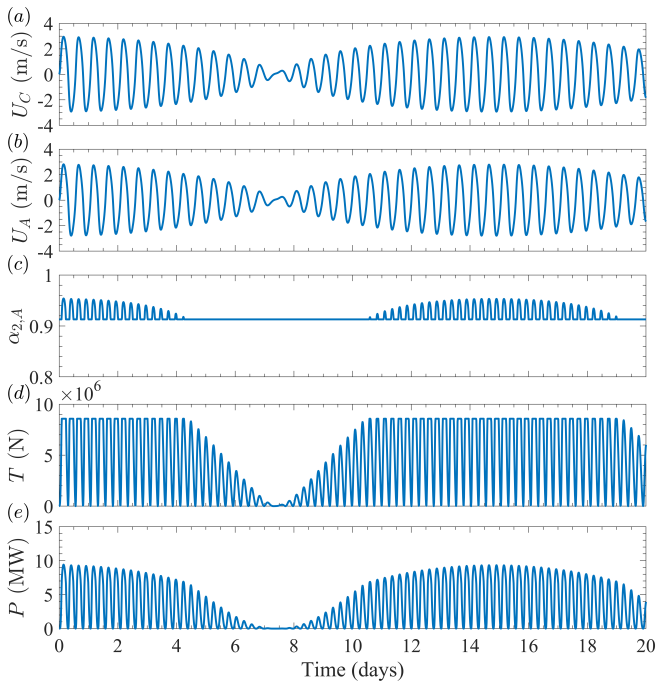


Fig. 2. Time history of channel velocity U_C (a), array velocity U_A (b), array induction factor α_A (c), thrust on the array T (d) and power (e), under the tidal forcing from the M2 and S2 constituents.

B. Variation of computational time with the number of tidal constituents

The computational time Δt increases significantly with increasing the number of tidal constituents N_C . Figure 3 shows the variation of computational time as the number of tidal constituents increases for the longest beat period among tidal constituents. Comparisons have been made on a laptop using 24 CPU cores. It is seen that with increasing the number of constituents from 1 to 4, the computational time increased by two orders of magnitude from 0.01 to 4.75 hours (Figure 3). While a run time of 4.75 hours might be acceptable in a standalone analysis, this computational time is very high when coupled with other design and optimisation algorithms. Therefore, it may be reasonable to focus on the two principal tidal constituents in order to balance computational efficiency and the accuracy.

V. CONCLUSIONS

In this paper, we propose a multi-scale framework for tidal resource assessment for the Co-Tide project. The key element of this framework is to model the system, i.e. an array of turbines (arranged in a row) partially occupying a tidal channel, at different scales (channel-scale, array-scale, turbine-scale), and then couple them together through the net resistance of the turbine array. The channel-scale flow dynamics is described by the Garrett & Cummins (2005) model [1] whereas based on the scale separation approach of Nishino & Willden (2012) [2] the array-scale and turbine-scale flows are modelled by Garrett & Cummins (2007) model [3] separately and then coupled together. To close the problem, a drag model is introduced, which establishes the relationship between

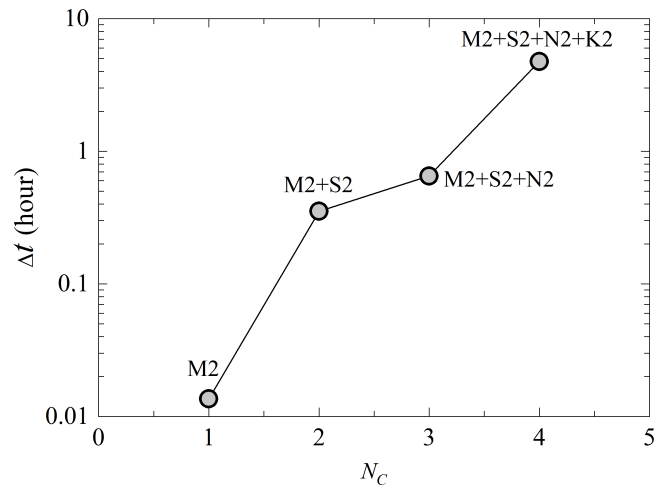


Fig. 3. Variation of computational time with increasing the number of tidal constituents. The periods for M2, S2, N2, and K2 are 12.42, 12.00, 12.66 and 11.97 hours, respectively.

the thrust on a turbine with the incident flow velocity. Integrating these four models results in a framework for tidal resource assessment for a row of turbines in a rectangular channel, based on tidal channel and turbine characteristics.

Using site characteristics informed by field data, we have employed the framework to predict the velocity in the channel, velocity through the array and the power generated by the array over time, considering two principal tidal constituents, M2, S2. It is demonstrated that the rated velocity in the drag model has significant influence on the channel-scale, array-scale and turbine-scale flow dynamics and hence power generation from neap to spring tides. Increasing the number of tidal constituents from 1 to 4 significantly increases the computational time to run the model by two orders of magnitude, partly due to the much longer simulation time required to capture the beat period between different constituent periods. For optimisation within a larger design and analysis model, focusing on two principal tidal constituents appears to be reasonable as it balances the computational costs and the accuracy of the results. It is possible to adopt this framework for other tidal energy projects.

REFERENCES

- [1] C. Garrett and P. Cummins, "The power potential of tidal currents in channels," *Proceedings of the royal society A: mathematical, physical and engineering sciences*, vol. 461, no. 2060, pp. 2563–2572, 2005.
- [2] T. Nishino and R. H. Willden, "The efficiency of an array of tidal turbines partially blocking a wide channel," *Journal of Fluid Mechanics*, vol. 708, pp. 596–606, 2012.
- [3] C. Garrett and P. Cummins, "The efficiency of a turbine in a tidal channel," *Journal of fluid mechanics*, vol. 588, pp. 243–251, 2007.
- [4] T. A. A. Adcock, S. Draper, R. H. J. Willden, and C. R. Vogel, "The fluid mechanics of tidal stream energy conversion," *Annual Review of Fluid Mechanics*, vol. 53, no. 1, pp. 287–310, 2021.
- [5] S. Draper, T. Stallard, P. Stansby, S. Way, and T. Adcock, "Laboratory scale experiments and preliminary modelling to investigate basin scale tidal stream energy extraction," in *Proceedings of the 10th European Wave and Tidal Energy Conference (EWTEC)*, Aalborg, Denmark, vol. 25, 2013.
- [6] L. S. Blunden and A. Bahaj, "Initial evaluation of tidal stream energy resources at Portland Bill, UK," *Renewable Energy*, vol. 31, no. 2, pp. 121–132, 2006.

- [7] R. Karsten, A. Swan, and J. Culina, "Assessment of arrays of in-stream tidal turbines in the Bay of Fundy," *Philosophical Transactions of the Royal Society A: Mathematical, Physical and Engineering Sciences*, vol. 371, no. 1985, p. 20120189, 2013.
- [8] J. Thiébot, P. B. Du Bois, and S. Guillou, "Numerical modeling of the effect of tidal stream turbines on the hydrodynamics and the sediment transport—Application to the Alderney Race (Raz Blanchard), France," *Renewable Energy*, vol. 75, pp. 356–365, 2015.
- [9] A. J. G. Brown, S. P. Neill, and M. J. Lewis, "Tidal energy extraction in three-dimensional ocean models," *Renewable Energy*, vol. 114, pp. 244–257, 2017.
- [10] R. O'Hara Murray and A. Gallego, "A modelling study of the tidal stream resource of the Pentland Firth, Scotland," *Renewable Energy*, vol. 102, pp. 326–340, 2017.
- [11] R. Vennell, "Tuning turbines in a tidal channel," *Journal of fluid mechanics*, vol. 663, pp. 253–267, 2010.
- [12] T. A. A. Adcock and S. Draper, "Power extraction from tidal channels—multiple tidal constituents, compound tides and over-tides," *Renewable Energy*, vol. 63, pp. 797–806, 2014.
- [13] R. Vennell and T. A. A. Adcock, "Energy storage inherent in large tidal turbine farms," *Proceedings of the Royal Society A: Mathematical, Physical and Engineering Sciences*, vol. 470, no. 2166, p. 20130580, 2014.
- [14] S. Muchala and R. H. J. Willden, "Influence of support structures on tidal turbine power output," *Journal of Fluids and Structures*, vol. 83, pp. 27–39, 2018.
- [15] L. Chen, P. A. Bonar, C. R. Vogel, and T. A. A. Adcock, "A note on the tuning of tidal turbines in channels," *Journal of Ocean Engineering and Marine Energy*, vol. 5, pp. 85–98, 2019.
- [16] T. A. A. Adcock, S. Draper, G. T. Houlsby, A. G. L. Borthwick, and S. Serhadloğlu, "The available power from tidal stream turbines in the Pentland Firth," *Proceedings of the Royal Society A: Mathematical, Physical and Engineering Sciences*, vol. 469, no. 2157, p. 20130072, 2013.
- [17] D. Dehtyriov, C. Vogel, and R. Willden, "A head-driven model of turbine fence performance," *Journal of Fluid Mechanics*, vol. 956, p. A14, 2023.
- [18] P. A. J. Bonar, L. Chen, A. M. Schnabl, V. Venugopal, A. G. Borthwick, and T. A. A. Adcock, "On the arrangement of tidal turbines in rough and oscillatory channel flow," *Journal of Fluid Mechanics*, vol. 865, pp. 790–810, 2019.
- [19] T. Nishino and R. H. Willden, "Two-scale dynamics of flow past a partial cross-stream array of tidal turbines," *Journal of Fluid Mechanics*, vol. 730, pp. 220–244, 2013.
- [20] F. W. Lanchester, "A contribution to the theory of propulsion and the screw propeller," *Journal of the American Society for Naval Engineers*, vol. 27, no. 2, pp. 509–510, 1915.
- [21] A. Betz, "Das maximum der theoretisch möglichen ausnützung des windes durch windmotoren," *Zeitschrift für das gesamte Turbinenwesen*, 1920.
- [22] N. Joukowsky, "Windmill of the nej type," *Transactions of the Central Institute for Aero-hydrodynamics of Moscow*, vol. 1, p. 57, 1920.
- [23] C. Vogel, G. Houlsby, and R. Willden, "Effect of free surface deformation on the extractable power of a finite width turbine array," *Renewable Energy*, vol. 88, pp. 317–324, 2016.
- [24] D. T. Pugh, "Tides, surges and mean sea-level (reprinted with corrections)," 1996.
- [25] K. Pappas, L. Mackie, I. Zilakos, A. H. van der Weijde, and A. Angeloudis, "Sensitivity of tidal range assessments to harmonic constituents and analysis timeframe," *Renewable Energy*, vol. 205, pp. 125–141, 2023.
- [26] T. A. A. Adcock, S. Draper, G. T. Houlsby, A. G. L. Borthwick, and S. Serhadloğlu, "Tidal stream power in the Pentland Firth—long-term variability, multiple constituents and capacity factor," *Proceedings of the Institution of Mechanical Engineers, Part A: Journal of Power and Energy*, vol. 228, no. 8, pp. 854–861, 2014.
- [27] J. Thiébot, N. Guillou, D. Coles, and S. Guillou, "On nodal modulations of tidal-stream energy resource in north-western Europe," *Applied Ocean Research*, vol. 121, p. 103091, 2022.